

Improvement Of Epitaxial Silicon Solar Cells On Upgraded Metallurgical Silicon By Heat Treatment

تحسين الخلايا الشمسية من السيليكون على سيليكون متالورجى مع
بواسطة المعالجة الحرارية

Roshdy A. Abderrassoul,
Electronic Eng. Dept., Mansoura University,
Mansoura, Egypt.

الخلاصة - تم تصليد سيليكون متالورجى معدل باستخدام الاستخلاص بواسطة الماء الملكى فى اتجاه واحد على الجرافيت ليعطى طبقات تحتية ذات مساحة كبيرة وجسيمات كبيرة ، وقبس تركيز الشوائب فى السيليكون باستخدام تكتيك بترسيب الامتصاص الذرى ، وأعدت خلايا شمسية ذات مساحة كبيرة (أكبر من 30 سم²) بترسيب وطلة موجب - سالب على الطبقات التحتية بواسطة الاختزال الحرارى لثالث كلوروسيلان ، وكانت كفاءة التحويل الجهد - ضوئى لها عند كتلة هواة (ك. ه.) (١) حوالى ٩ فى المائة . وقبست خصائص الخلايا الشمسية بقياسات التيار - جهد المظلم والمضاء ، الاستجابة الطيفية ، وطول الانتشار لحاملات الشحنة الأقلية واستعمال ميكروسكوب المسح الألكترونى وتكتيك التيار الممتحك بالشعاع الألكترونى . ودرسنا تأثير المعالجة الحرارية على هذه البارامترات . وقبست وحد أن المعالجة الحرارية فى جو خامل تحسن من خصائص الخلايا الشمسية ، ويفترض أن ذلك نتيجة لانتشار الشوائب المعدنية الموجودة فى الطبقة التحتية وفى الطبقات الناعمة الى حدود الجسيمات .

Abstract : Metallurgical - grade silicon upgraded by aqua - regia extraction was unidirectionally solidified on graphite to yield large - area large - grain substrates. The concentration of impurities in the silicon substrates was measured using the atomic absorption technique. Epitaxial silicon layers were deposited on the metallurgical silicon substrate by the thermal reduction of trichlorosilane. Heat treatment in an inert atmosphere was found to improve the characteristics of the solar cells, presumably due to the diffusion of metallic impurities in the substrate and the epitaxial layers to the grain boundaries. Large - area (more than 30 cm²) solar cells, having an air mass one (AM1) photovoltaic conversion efficiency of 9 %, were prepared by depositing a p - n junction epitaxially onto the metallurgical silicon substrate. The solar cells were characterized by darkcurrent - voltage, illuminated current - voltage, spectral response and minority carrier diffusion length measurements, and SEM and EBIC (electron - beam induced current) techniques. The effect of heat treatment on these parameters was studied.

I. Introduction :

Metallurgical - grade silicon having a purity of about 98% is an attractive starting material for low cost silicon solar cells. The use of metallurgical silicon for solar cell fabrication has been studied by several investigators [1-4]. Epitaxial silicon layers of controlled thickness and dopant concentration deposited on metallurgical silicon substrates have been shown to be a promising photovoltaic material [5]. Impurities in metallurgical silicon must be removed as completely as possible using low cost techniques, since most metallic impurities, particularly titanium, vanadium, and zirconium, have been shown to significantly reduce the minority carrier lifetime in single crystal silicon [6,7]. Furthermore, the metallurgical silicon substrate must have relatively large grains, since silicon is an indirect bandgap semiconductor with a gradual absorption edge, and since large grains are required to achieve reasonable photovoltaic collection efficiencies.

Metallurgical silicon contains iron and aluminum as the major impurities at concentrations of a few tenths of a per cent; other impurities include boron, chromium, copper, manganese, nickel, titanium, vanadium, zirconium, etc., at concentrations up to several hundred parts per million. The purification of metallurgical silicon in the semiconductor industry involves the trichlorosilane intermediate, and is energy intensive and cost ineffective.

Several direct purification techniques, such as acid extraction [8], gettering [9], and the treatment of the melt with reactive gases [10,11], have been reported. Although none of these techniques is completely effective, each has its own merit. In this paper, acid extraction was used for the partial purification of metallurgical silicon because of its simplicity and low energy requirement. The partially purified material was made into a large grain substrate by melting and unidirectional solidification on graphite. Thermal reduction of trichlorosilane by hydrogen containing appropriate dopants was used for the epitaxial deposition of the active layers of the solar cells. Heat treatment was found to significantly enhance the solar cell characteristics, as shown by measuring the photovoltaic

conversion characteristics of the cells and by the electron - beam induced current (EBIC) technique, presumably due to the diffusion of the metallic impurities in the substrate and in the epitaxial layer to the grain boundaries,

II. Acid Extraction of metallurgical silicon :

Many metallic impurities such as iron, aluminum, copper, gold, nickel, titanium, .. etc., are highly soluble in molten silicon, while their solubilities in solid silicon are relatively low [12]. Thus, during the solidification of molten metallurgical silicon during the manufacturing process, the majority of these impurities should precipitate at grain boundaries or at interstitial positions, presumably in the form of silicides or other compounds. The pulverization of the cast metallurgical silicon generally takes place at grain boundaries and the small grains (1 - 2 mm, for example) are either single crystals or aggregates of two or three crystals [1]. Therefore the majority of the metallic impurities are concentrated at the surface of the grains, and treatment of the pulverized metallurgical silicon with acids should be effective in the removal of these impurities, as well as the impurities inside the grains. However, the dissolution of the impurities was found to be a slow process and impurities within the grains cannot be removed.

Table (1) shows the concentration of impurities in as - received pulverized metallurgical grade silicon, determined by atomic absorption analysis. Aqua regia was found to be more effective than hydrochloric acid or sulfuric acid in the extraction of metallic impurities from pulverized metallurgical silicon [8].

Table (1). Concentration of impurities in as - received metallurgical silicon and metallurgical silicon purified by aqua - regia extraction determined by atomic absorption analysis.

Element	Concentration (at. ppm)	
	As-received metallurgical silicon	Metallurgical silicon after aqua - regia treatment
Al	610	320
Cu	10	5
Fe	1500	350
Mn	40	10
Ni	25	15

The concentration of iron in pulverized metallurgical silicon after aqua regia treatment was found by the atomic absorption analysis to have reduced to 350 (at. ppm) [13]. It is expected that concentrations of other metallic harmful impurities, such as aluminum, would also be significantly reduced after acid extraction.

Acid - treated pulverized metallurgical silicon was uniformly spread on the top of a 28 cm x 7.5 cm x 1.5 cm graphite plate, the surface of which was roughened by sandblasting to increase the Si - substrate interfacial tension. The graphite plate was loaded into a fused silica tube of an inside diameter of 10.5 cm in a helium atmosphere, and was rf heated by induction using a 450 kHz rf source. The temperature profile along the graphite plate was controlled by adjusting the spacings between the turns of the rf coil so as to yield a temperature gradient of 80 - 100 °C along the length of the substrate. The entire silicon charge was first melted, then the rf power was reduced so that unidirectional solidification started from one end of the substrate to the other. The solidification

was initiated from the surface of the melt and proceeded inwards, in order to minimize the crystallographic orienting effects of polycrystalline graphite. The thermal conditions were controlled so as to yield a planar solid - liquid interface during the solidification process, resulting in elongated crystallites, several centimeters long. The rate of solidification is the most important parameter affecting the morphology of the unidirectionally solidified material. High solidification rates (e.g. 5 cm/min) resulted in non - planar surfaces, with many ridges, faces, and valleys. Lower solidification rates (e.g. 1 - 2 cm/min) resulted in planar surfaces. X-ray diffraction examinations of the planar material indicate that the majority of the crystallites are of $\{110\}$ orientation. Grain boundaries, multiple twins, and dislocations are the major crystallographic defects in the unidirectionally - solidified metallurgical silicon substrates.

III. Heat treatment of metallurgical silicon substrates :

Metallurgical silicon substrates were subjected to heat treatment in an inert atmosphere, such as helium, at 700 °C for various durations. In all cases the concentration of metallic impurities at grain boundaries was found to increase appreciably [14]. Thus the grain boundaries serve as a sink for the precipitation of metallic impurities, and the presence of grain boundaries may be considered as an advantage when using chemically upgraded metallurgical silicon for solar cell purposes [15]. Segregated impurities at grain boundaries may affect trapping and surface recombination; however, such effects will not appreciably alter the extent of carrier recombination at grain boundaries and therefore the photocurrent and photovoltage will not be changed.

IV. Epitaxial silicon solar cells :

Epitaxial silicon films were deposited on silicon

substrates, prepared by the unidirectional solidification of aqua - regia treated metallurgical silicon on graphite, using the thermal reduction of trichlorosilane by hydrogen. The substrate was placed in a fused silica tube of inside diameter 10.5 cm and heated externally using an r.f. generator. *In situ* etching of the substrate with a mixture of hydrogen and hydrogen chloride at 1200 °C was used to remove 2 - 3 μm of silicon from the substrate surface. Silicon was then epitaxially deposited at 1100 °C. The substrate is always p type having a resistivity of 0.04 - 0.06 Ω.cm. Successive deposition of p- and n - type silicon films was used to produce a thin film solar cell. The p layer had a resistivity of 0.2 - 0.5 Ω.cm and was 20 - 25 μm thick, while the n layer was 2 μm thick and had a resistivity graded from 2×10^{-4} to 4×10^{-3} Ω.cm. After the deposition the solar cells were heated in helium at 700 °C to allow the diffusion of metallic impurities to grain boundaries. The grid contact was then applied to the front surface of the cell by evaporating 1000 Å of titanium followed by 2 - 3 μm of silver through a metal mask, and then annealing in hydrogen at 500 °C. The graphite plate served as the back contact. Tin oxide antireflective (AR) coating was applied by the oxidation of tetramethyltin in an argon atmosphere.

The solar cells were characterized by current - voltage and spectral response measurements. Figure 1 shows the current - voltage characteristics of a thin film silicon solar cell of area 37 cm² under illumination with quartz - halogen lamps at air mass one (AM1) conditions. The open - circuit voltage, V_{oc} , short - circuit current density, J_{sc} , and fillfactor FF are 0.57 V, 20.8 mA/cm², and 75.6%, respectively, corresponding to an AM1 efficiency of 8.95%. The heat treatment was found to increase the photovoltage and photocurrent by up to 5% and 10%, respectively, and thus to increase the photovoltaic conversion efficiency by up to 20%.

The spectral response of the cell was measured at a set of discrete wavelengths selected using interference filters, and a calibrated single - crystal silicon solar cell of area 4 cm² was used as a reference. Figure 2 shows the spectral response of the same solar cell, compared with that of the calibrated cell. The peak response of the polycrystalline cell occurs at a shorter wavelength than that of the single crystal cell. In addition, the quantum

efficiency in the polycrystalline cell is lower than that in the single crystal cell. The shift in the peak response and the lower quantum efficiency are not unexpected in view of the small thickness of the active region of the polycrystalline cell and the short minority carrier diffusion length in the cell.

V. Results :

Figure 3.a shows an SEM picture of a non - annealed silicon solar cell, and figure 3.b shows an EBIC (Electron Beam Induced Current) picture of the same cell. It is clear that grain boundaries represent the major defects in the material that cause carrier recombination. Figure 4.a shows an EBIC picture- and figure 4.b shows a line scan picture along line AA of a polycrystalline silicon solar cell that was heat - treated at 850 °C, while figure 4.c is for a line scan BB of the same cell. The deleterious effects of the grain boundaries on the response are clear, causing a sharp reduction in the EBIC signal, whereas twin planes don't show that serious effect. Figure 5 shows an EBIC picture and a line scan picture along line AA of a solar cell that was annealed at 950 °C.

Figure 6 shows the effect of annealing on the diode quality factor, n_1 , of the solar cells. In figure 7, the effect of annealing on the minority carrier diffusion length in the base layer of the cell, determined by the surface photovoltage (SPV) method [16] is shown. Figure 8 shows the effect of the annealing condition on the open - circuit voltage and the short - circuit current density of the cells. From this figure it is apparent that annealing at 850 °C is preferable to that at 950 °C. Figure 9 shows the effect of annealing on the spectral response of the polycrystalline cells.

VI. Conclusions :

In this work we investigate the effect of heat treatment on polycrystalline silicon thin film solar cells made on acid - treatment upgraded metallurgical grade silicon on graphite by chemical vapor deposition. Heat treatment is found to improve the performance of the solar cells.

Further research is required to determine the mechanism of this improvement and the optimum annealing conditions.

References :

1. L. P. Hunt, V. D. Dosaj, J. R. McCormick, and L. D. Crossman, *Proc. of the Int. Symp. on Solar Energy*, (1976), 200.
2. T. Saitoh, T. Warabisako, E. Kuroda, H. Itoh, S. Matsubara, and T. Tokuyama, *IEEE Trans. Electron Devices*, 27(1980), 671.
3. J. I. Hanoka, H. B. Strock, and P. S. Kotval, *J. Appl. Phys.*, 52(1981), 5829.
4. R. V. D'Aiello, P. H. Robinson, and E. A. Miller, *RCA Review*, 44(1983), 30.
5. T. L. Chu and K. N. Singh, *Solid-State Electron.*, 19(1976), 837.
6. J. R. Davis, A. Rohatgi, P. Rai-Choudhury, P. Blais, R. H. Hopkins and J. R. McCormick, *Proc. 13th IEEE Photovoltaic Specialists' Conf.*, Washington, D.C., June 5 - 8, 1978, p. 490.
7. G. F. Wakefield, P. D. Maysock, and T. L. Chu, *Proc. 11th IEEE Photovoltaic Specialists' Conf.*, Scottsdale, Arizona, May 6 - 8, 1975, p. 49.
8. W. Voos, *U.S. Patent 2,972,521*, Feb. 21, 1961.
9. C. J. Brockbank, *U.S. Patent 1,180,968*, April 25, 1916.
10. E. Enk and J. Nickl, *Ger. Patent 1,098,931*; *Chem. Abstr.*, 56(1960) 5633.
11. T. L. Chu, G. A. Van der Leeden and H. I. Yoo, *J. Electrochem. Soc.*, 125(1979) 661.

12. F. A. Trumbore, *Bell Syst. Tech. J.*, 39(1960) 205.
13. T. L. Chu, E. D. Stokes, and R. A. Abderrassoul, *Proc. IEEE 1989 Southeastcon*, Clemson, S.C., April 9 - 12, 1989, p. 1436.
14. T. Saito, M. Fujisaki, N. Mizukami, M. Geshi, T. Yamada, and K. Tabata, *Tech. Digest of the Intl. PVSEC-1*, Kobe, Japan, 1984, p. 801.
15. T. Warabisko, T. Saitoh, E. Kuroda, H. Itoh, N. Nakamura, and T. Tokuyama, *Jpn. J. Appl. Phys.*, 19(1980) 539.
16. T. L. Chu and E. D. Stokes, *Proc. IEEE 13th Photovoltaic Specialists' Conf.*, Washington, D.C., June 5 - 8, 1978, p. 95.

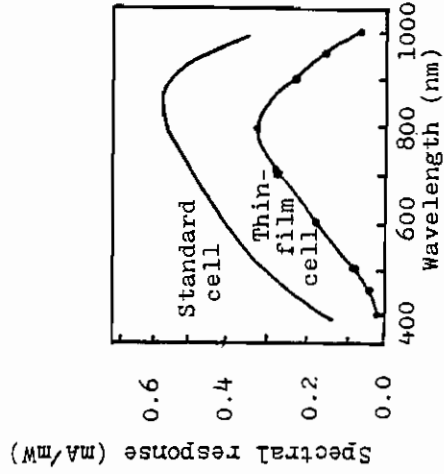


Figure 2. The spectral response of the cell shown in Fig. 1, compared to a single crystalline standard silicon solar cell.

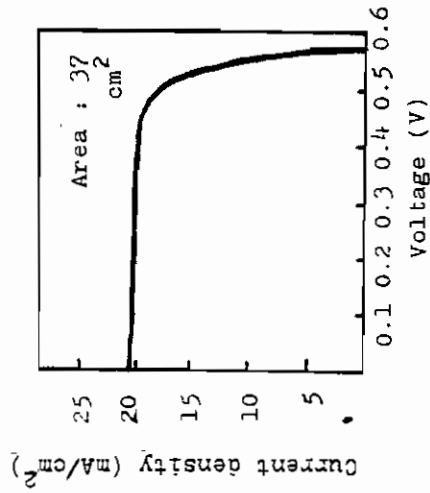


Figure 1. Current-voltage characteristics of a polycrystalline silicon solar cell under AM1 conditions.



b) EBIC picture



a) SEM picture

Figure 3. Scanning electron microscope and EBIC pictures of a non annealed polycrystalline silicon solar cell (# 121)

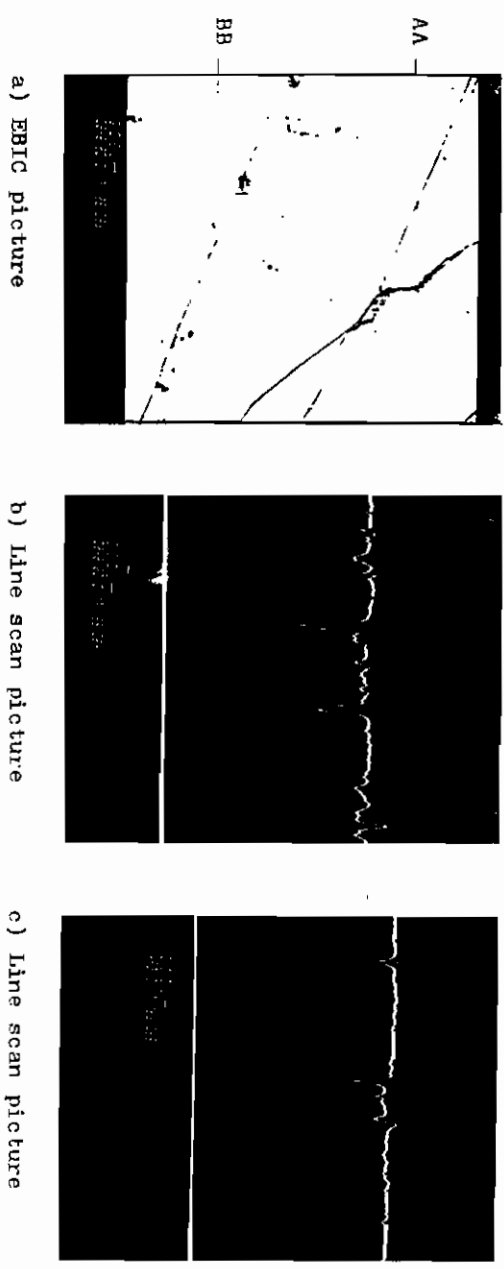
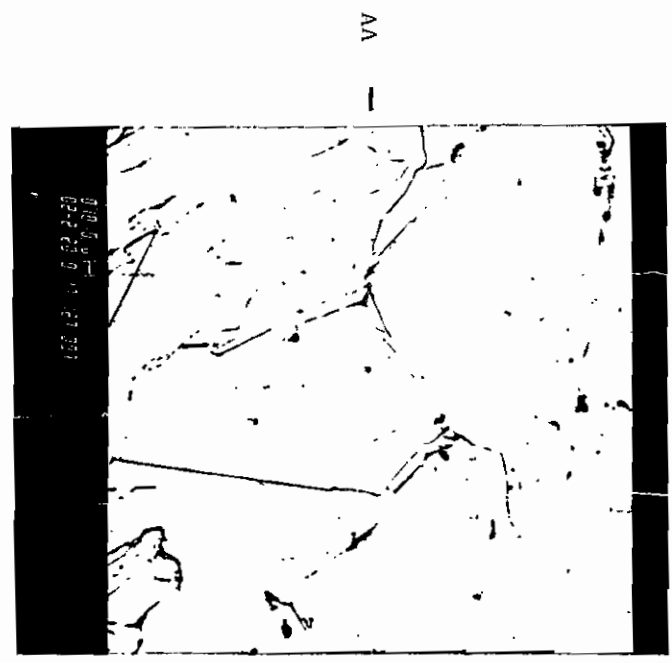


Figure 4. EBIC and line scan pictures for a cell annealed at 850 °C (# 122)

a) EBIC picture



b) Line scan picture along line AA

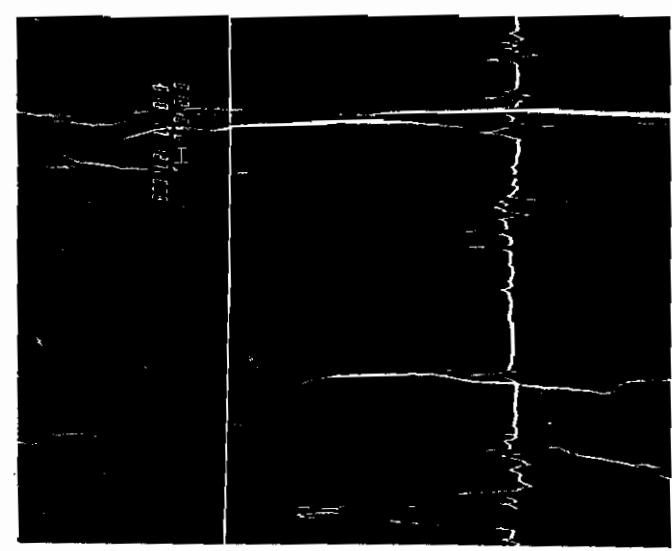


Figure 5. EBIC and line scan pictures of a polycrystalline silicon solar cell annealed at 950 °C (# 123)

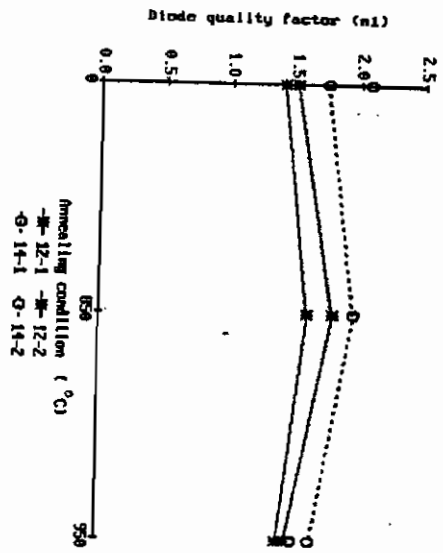


Figure 6. The effect of annealing on the diode quality factor

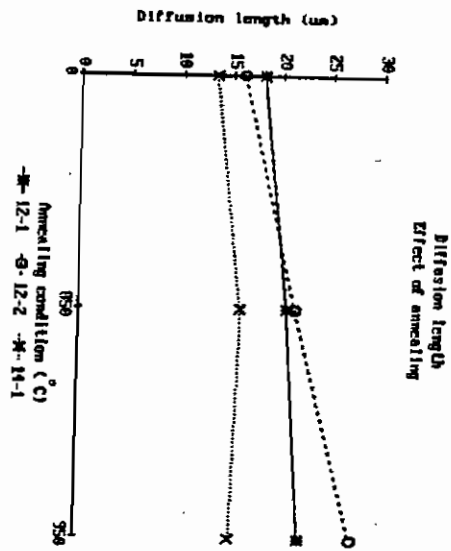
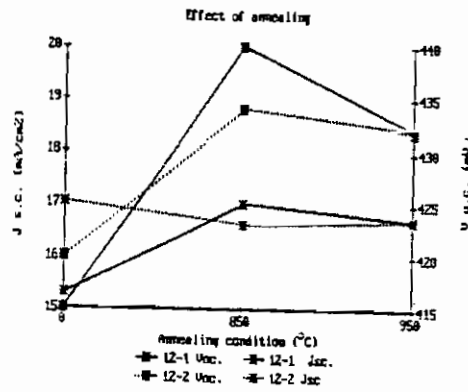
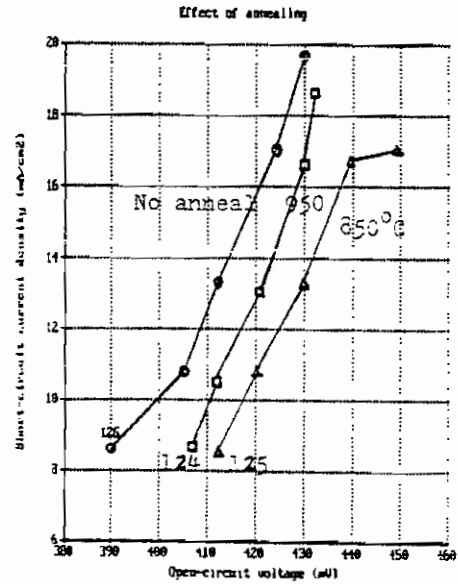
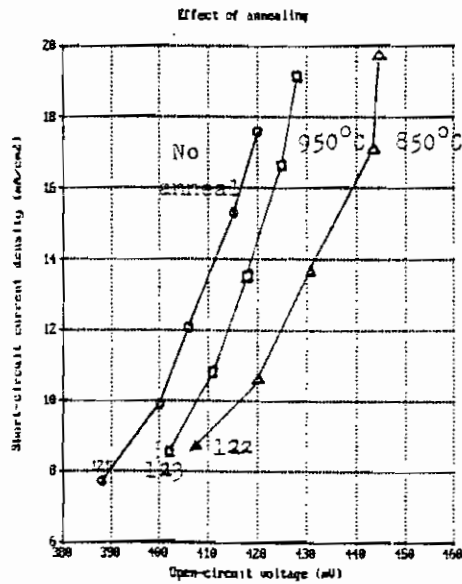


Figure 7. The effect of annealing on the minority carrier diffusion length



a) Effect of annealing on V_{oc} and I_{sc}



b) I_{sc} vs V_{oc} for samples 12-1

c) I_{sc} vs V_{oc} for samples 12-2

Figure 8. The effect of annealing on the open-circuit voltage and the short-circuit current density of polycrystalline silicon solar cells.

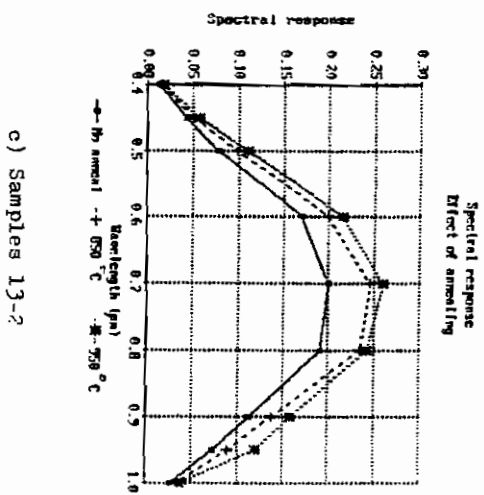
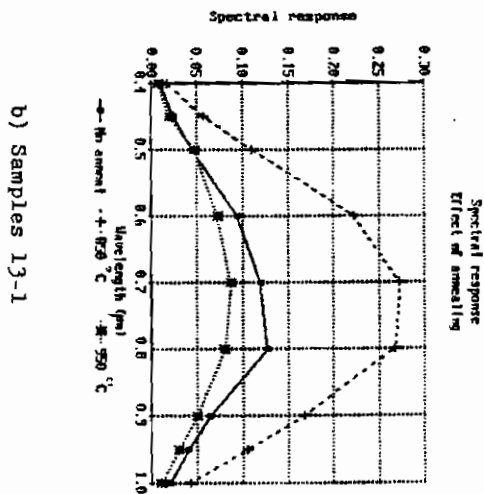
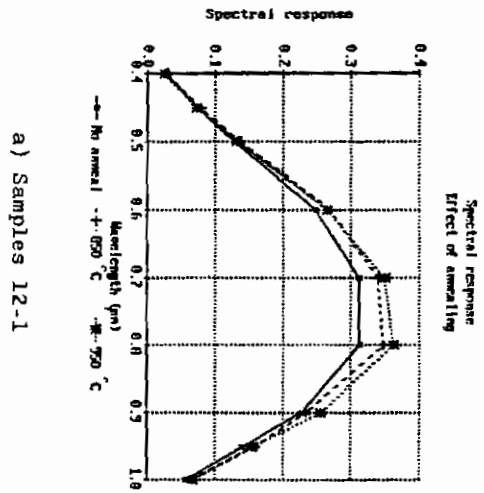


Figure 9. The effect of annealing on the spectral response of polycrystalline silicon solar cells